Physical realizations and Wigner representation of coherent states of finite-dimensional Hilbert spaces

ADAM MIRANOWICZ[1-3], ŞAHIN K. ÖZDEMIR[1,2], YU-XI LIU[2],
MASATO KOASHI[1,2], AND NOBUYUKI IMOTO[1,2,4,5]

[1] *CREST Research Team for Interacting Carrier Electronics, Japan Science and Technology Corporation, Hayama, Kanagawa 240-0193, Japan*

[2] *School of Advanced Sciences, Graduate University for Advanced Studies (SOKEN), Hayama, Kanagawa 240-0193, Japan*

[3] *Nonlinear Optics Division, Institute of Physics, Adam Mickiewicz University, 61-614 Poznań, Poland*

[4] *University of Tokyo, 7-3-1 Hongo, Bunkyo-ku, Tokyo 113-8654, Japan*

[5] *NTT Basic Research Laboratories, 3-1 Morinosato Wakamiya, Atsugi, Kanagawa 243-0198, Japan*

Two essentially different mathematical approaches to define coherent states of finite-dimensional Hilbert spaces are analyzed. Physical realizations of the so-called quantum scissors to generate the finite-dimensional states via optical truncation are discussed including the linear-optical scheme of Pegg, Phillips and Barnett [Phys. Rev. Lett. **81**, 1604 (1998)] and nonlinear one of Leoński and Tanaś [Phys. Rev. A **49**, R20 (1994)]. Distinct properties of the generated states are studied by applying a discrete Wigner function.

I. INTRODUCTION

In 1931, Weyl's formulation of quantum mechanics [1] opened a possibility of studying the dynamics of quantum systems in finite-dimensional (FD) Hilbert spaces of operators which are bounded and have a discrete spectrum. In 1960, Schwinger [2], by generalizing Weyl's formulation, triggered a new interest to investigate harmonic-oscillator states defined in FD Hilbert spaces including contributions of Radcliffe [3], Perelomov [4], Arecchi *et al.* [5], Gilmore *et al.* [6,7], Santhanam *et al.* [8], and Glauber and Haake [9] to construct analogs of the conventional optical coherent states [10,11]. In the last decade, the interest in the FD quantum-optical states has been stimulated by the progress in quantum-optical state preparation and measurement techniques [12], in particular, by the development of the discrete quantum-state tomography [13] and quantum information with optical qubits.

Various quantum-optical states were constructed in FD Hilbert spaces in analogy to those in the infinite-dimensional (ID) spaces (for a review see [14]). In particular, special interest has been paid to FD coherent states (CS) [15–19]. As was shown in [14], two kinds of FD coherent states can be distinguished as corresponding to their generation by applying different truncation schemes, referred to as the so-called *quantum scissors*. One of them is related to truncation of the photon-number expansion of the optical state as proposed by Pegg, Phillips and Barnett (PPB) [20] and then generalized by others [21–23]. Thus, we shall refer to these states as the *PPB-truncated* states. Alternatively, one can analyze states obtained by a direct truncation of operators rather than that of their Fock expansion. Such an operator-truncation scheme was proposed by Leoński and Tanaś (LT) [24-27] (for a review see [28]). Thus, the states generated by this scheme can be called the *LT-truncated*

states. In order to describe essential differences between the PPB- and LT-truncated states, we apply a discrete Wigner function.

Wigner function is widely used in nonrelativistic quantum mechanics as an alternative to the density matrix of quantum systems [29]. Although the original Wigner function applies only to systems with continuous degrees of freedom, it can be generalized for finite-state systems as well [30]. Discrete Wigner function for spin-$\frac{1}{2}$ systems was introduced by O'Connell and Wigner [31] and generalized for arbitrary spins by Wootters [32]. Wootters' definition takes the simplest form for prime-number-dimensional systems. A similar construction of a discrete Wigner function for odd-dimensional systems was suggested by Cohendet et al. [33]. A number-phase discrete Wigner function, a special case of the Wootters definition, was analyzed in detail by Vaccaro and Pegg [34]. Another definition of Wigner function (for odd dimensions equivalent to that of Wootters) was proposed by Leonhardt [13]. The Wigner function approach to FD systems can be developed from basic principles as was shown, for example, by Hannay and Berry [36], Wootters [32], Leonhardt [13], Lukš and Peřinová [35], or Luis and Peřina [37]. Discrete Wigner function has successfully been applied to quantum-state tomography of FD systems [13].

In Sect. II, we present formal approaches to study states and their Wigner-function representation for finite-dimensional Hilbert spaces. In Sect. III, we discuss physical implementations of truncation schemes to generate FD coherent states and present Wigner functions of the generated states.

II. FD OPTICAL STATES AND THEIR WIGNER REPRESENTATION

Finite (say, $s+1$) dimensional Hilbert space, denoted by $\mathcal{H}^{(s)}$, can be spanned by number states $\{|0\rangle, |1\rangle, \ldots, |s\rangle\}$ fulfilling the relations of completeness, $\hat{1}_s = \sum_{n=0}^{s} |n\rangle\langle n|$, and orthogonality, $\langle n|m\rangle = \delta_{n,m}$, for $n, m = 0, \ldots, s$. Here, $\hat{1}_s$ denotes the $(s+1)$-dimensional identity operator. Arbitrary quantum-optical pure state in the FD Hilbert space can be defined by its Fock expansion

$$|\psi\rangle_{(s)} = \sum_{n=0}^{s} b_n^{(s)} e^{i\varphi_n} |n\rangle, \qquad (1)$$

where $b_n^{(s)}$ are real superposition coefficients fulfilling the normalization condition $_{(s)}\langle\psi|\psi\rangle_{(s)} = \sum_{n=0}^{s} [b_n^{(s)}]^2 = 1$. The FD annihilation and creation operators in $\mathcal{H}^{(s)}$ are defined by

$$\hat{a}_s = \sum_{n=1}^{s} \sqrt{n}|n-1\rangle\langle n|, \quad \hat{a}_s^\dagger = \sum_{n=1}^{s} \sqrt{n}|n\rangle\langle n-1|. \qquad (2)$$

The FD and ID annihilation operators act on a number state in the same manner. However, the actions of the creation operators on $|n\rangle$ are different in $\mathcal{H}^{(s)}$ and $\mathcal{H}^{(\infty)}$. Equation (2) implies that $(\hat{a}_s^\dagger)^k |n\rangle = 0$ if $n+k > s$. By contrast, the action of the ID creation operator (in any power) on $|n\rangle$ gives always nonzero result. The commutation relation for the annihilation and creation operators in $\mathcal{H}^{(s)}$ reads as

$$[\hat{a}_s, \hat{a}_s^\dagger] = 1 - (s+1)|s\rangle\langle s|, \qquad (3)$$

which differs from the conventional boson canonical relation in $\mathcal{H}^{(\infty)}$. Even double commutators $[\hat{a}_s, [\hat{a}_s, \hat{a}_s^\dagger]]$ and $[\hat{a}_s^\dagger, [\hat{a}_s, \hat{a}_s^\dagger]]$ do not vanish precluding the application of the Baker-Hausdorff theorem. These properties of the FD annihilation and creation operators considerably complicate analytical approaches to the quantum mechanics in $\mathcal{H}^{(s)}$, including the explicit construction of the FD harmonic oscillator states.

Instead of number-state representation, the FD Hilbert space can also be spanned the phase states defined to be [38]:

$$|\theta_m\rangle \equiv |\theta_m\rangle_{(s)} = \frac{1}{\sqrt{s+1}} \sum_{n=0}^{s} \exp(in\theta_m)|n\rangle, \tag{4}$$

where $\theta_m = \theta_0 + \frac{2\pi}{s+1} m$ with θ_0 being the initial reference phase and $m = 0, \ldots, s$. The phase states, same as number states, form a complete, $\hat{1}_s = \sum_{m=0}^{s} |\theta_m\rangle\langle\theta_m|$, and orthonormal, $\langle\theta_m|\theta_n\rangle = \delta_{m,n}$, basis. Thus, the FD optical states, given by (1), can alternatively be defined by their phase-state expansion as $|\psi\rangle_{(s)} = \sum_{m=0}^{s} d_m^{(s)} e^{i\phi_n} |\theta_m\rangle$ with superposition coefficients normalized to $\sum_{m=0}^{s} [d_m^{(s)}]^2 = 1$. Formulas similar to Eqs. (2) and (3) were formulated for the phase states too (for details see [15,14]).

The number–phase characteristic function in $\mathcal{H}^{(s)}$ can be defined as [13]

$$C_s(\nu, \theta_\mu) = \sum_{m=0}^{s} \exp\left(-\frac{4\pi i}{s+1}\nu(m+\mu)\right) \langle\theta_m|\hat{\rho}|\theta_{m+2\mu}\rangle \tag{5}$$

in terms of the phase states (4), while the phase θ_μ in l.h.s. is determined by θ_0 and the index μ in r.h.s. of (5). A discrete Fourier transform applied to $C_s(\nu, \theta_\mu)$ leads to the following discrete Wigner function (for brevity referred to as the W function) for phase and number

$$W_s(n, \theta_m) = \frac{1}{(s+1)^2} \sum_{\nu=0}^{s} \sum_{\mu=0}^{s} \exp\left(\frac{4\pi i}{s+1}(n\mu + \nu m)\right) C_s(\nu, \theta_\mu) \tag{6}$$

or, explicitly, as [32,13]

$$W_s(n, \theta_m) = \frac{1}{s+1} \sum_{\mu=0}^{s} \exp\left(\frac{4\pi i}{s+1}n\mu\right) \langle\theta_{m-\mu}|\hat{\rho}|\theta_{m+\mu}\rangle. \tag{7}$$

The Wigner function $W_s(n, \theta_m)$ is periodic both in n and θ_m:

$$W_s(n, \theta_m) = W_s(n \pm \{s+1\}, \theta_m) = W_s(n, \theta_{m\pm(s+1)}) = W_s(n, \theta_m \pm 2\pi). \tag{8}$$

Thus, it is represented graphically on torus [18,14]. The Wigner function for any FD pure state of the form (1) can be expressed as follows [34]

$$W_s(n, \theta_m) = \frac{1}{s+1} \left\{ \sum_{k=0}^{M} b_k^{(s)} b_{M-k}^{(s)} \exp[i(2k - M)\theta_m + \varphi_{M-k} - \varphi_k] \right.$$
$$\left. + \sum_{k=M+1}^{s} b_k^{(s)} b_{M-k+s+1}^{(s)} \exp[i(2k - M - s - 1)\theta_m + \varphi_{M-k+s+1} - \varphi_k] \right\} \tag{9}$$

in terms of the decomposition coefficients $b_k^{(s)}$ and $M \equiv 2n \bmod(s+1)$. The physical interpretation of the Wigner functions is based on the fact that the marginal sum of their values

over a generalized line gives the probability of finding the system in a given state [32,13]. In the ID Hilbert space, where the W function arguments are continuous (quadratures X and Y), a marginal integral along any straight line $aX + bY + c = 0$ is nonnegative and can be considered to be the probability. A similar situation arises in the FD case; we can define lines as sets of discrete points (n, θ_m), or equivalently (n, m), for which the relation $(an + bm + c)\mathrm{mod} N = 0$ holds (here, a, b, c are integers). Again, sums of the discrete W function values on such sets are nonnegative. The mod $(s + 1)$ relations are essential and are connected to some periodic properties of the discrete W function — the maximum value of each argument (m or n) is topologically followed by its minimum (zero in our case). This means that the discrete W function is defined on a torus (or more precisely on a discrete set of points of a torus). The "lines" are then points of closed toroidal spirals or, in a special case, points of a circle. The periodic property is quite natural for the phase index m, but may seem strange for the photon number n. Because of the discreteness of the arguments, the W function graph should be a histogram. However, two-dimensional projections of such three-dimensional histograms could be very confusing. Therefore, for better legibility of the graphs, we have decided to depict them topographically. The darker is a region, the higher is the value of the W function it represents. Moreover, negative values of the W function are marked by crosses. As mentioned above, the most natural way of presenting the discrete W function graphs is to construct them on toruses. A few simple examples of the toroidal discrete Wigner functions are given in [14]. Unfortunately, this graphical representation is seldom transparent enough for its interpretation. In what follows we shall work with two-dimensional graphs. Here, one should keep in mind that some consequences of the periodicity in n and m can appear: for instance, some peaks can be located partially at the outer boundary at $n \approx s$ (or $m \approx s$) and can "continue" near the center $n \approx 0$ (or $m \approx 0$).

III. GENERATION OF FD COHERENT STATES BY QUANTUM SCISSORS

Glauber coherent states in infinite-dimensional Hilbert space can be defined in various equivalent ways [10,7], e.g., by the action of the displacement operator on vacuum state:

$$|\alpha\rangle = \exp(\alpha \hat{a}^\dagger - \alpha^* \hat{a})|0\rangle, \tag{10}$$

where the annihilation and creation operators are, respectively,

$$\hat{a} = \sum_{n=1}^{\infty} \sqrt{n}|n-1\rangle\langle n|, \quad \hat{a}^\dagger = \sum_{n=1}^{\infty} \sqrt{n}|n\rangle\langle n-1|. \tag{11}$$

By applying the Baker-Hausdorff identity to (10), one obtains the well-known equivalent definition

$$|\alpha\rangle = \exp(-\frac{1}{2}|\alpha|^2) \sum_{n=0}^{\infty} \frac{\alpha^n}{\sqrt{n!}}|n\rangle \tag{12}$$

based on explicit Fock expansion. However, in FD Hilbert space, definitions (10) and (12) are by no means equivalent. In the following, we show that the truncation of the sum in (12) leads to the PPB-truncated coherent states, while the truncation of annihilation and creation operators in (10) corresponds to the LT-truncated coherent states.
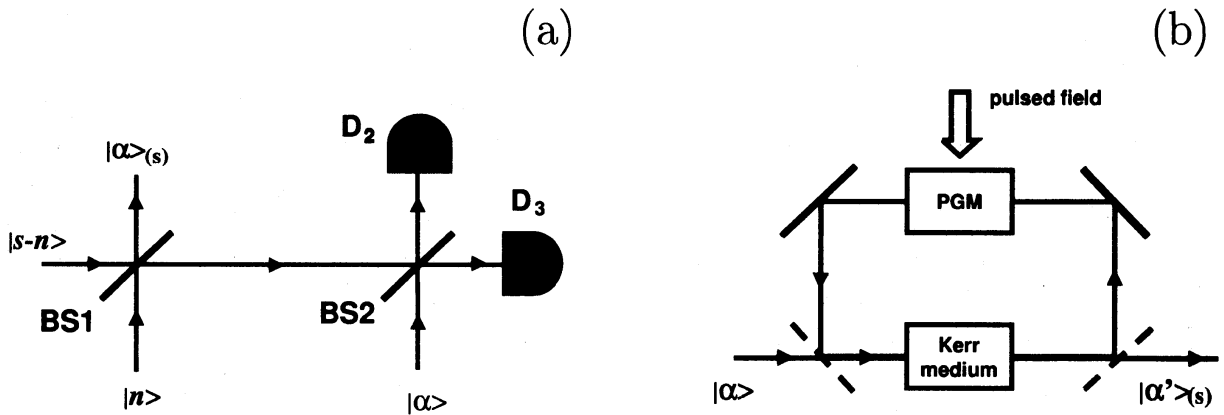
(a)

(b)

FIG. 1. Schemes of two kinds of quantum scissors according to (a) Pegg, Phillips, and Barnett (PPB) and (b) Leoński and Tanaś (LT). Key: $|\alpha\rangle$ – input coherent states; $|\alpha\rangle_{(s)}$ – PPB-truncated coherent states; $|\alpha'\rangle_{(s)}$ – LT-truncated coherent states; $|n\rangle$ and $|s - n\rangle$ – input photon-number states; if $s=1$ than $n=0$ or 1, and if $s=2$ than $n=1$; D_2, D_3 – photon-counting detectors; BS1, BS2 – beam splitters; PGM – parametric gain medium.
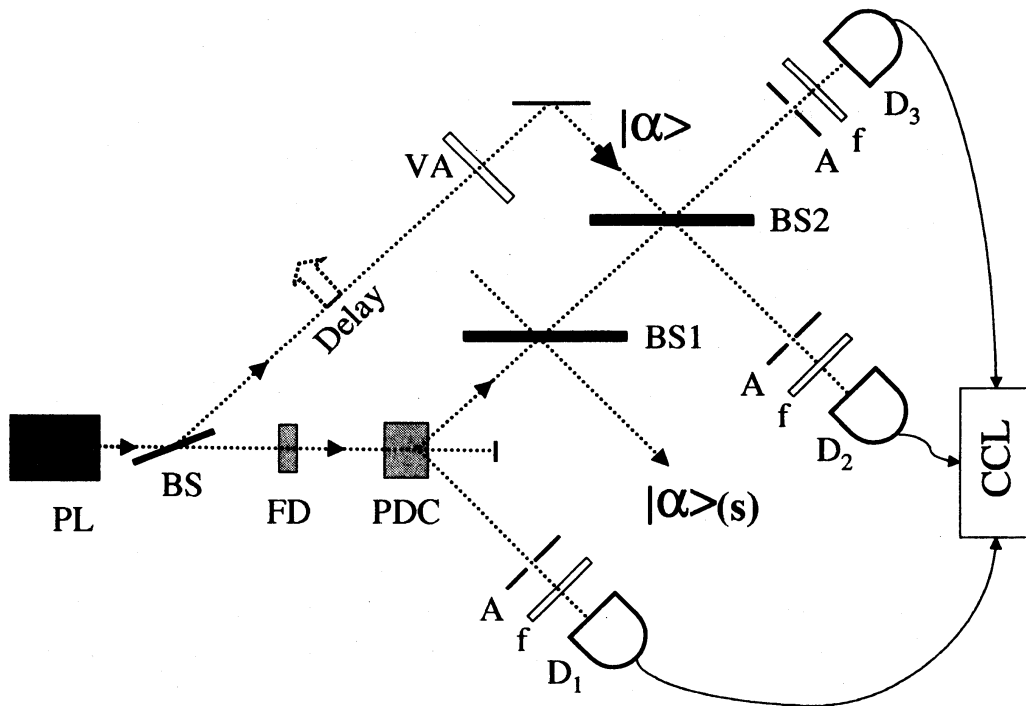

FIG. 2. Scheme of experimental realization of the PPB quantum scissors corresponding to Fig. 1(a). Key: PL – pulsed laser; FD – frequency doubler; PDC – parametric down conversion crystal; VA – variable attenuator; A – aperture; f – narrow band filter; CCL – coincidence counter and logic; BS, BS1, and BS2 – beam splitters; and D_1, D_2, and D_3 – photon-counting detectors.

A. QUANTUM SCISSORS OF PEGG, PHILLIPS AND BARNETT

The optical truncation scheme (quantum scissors) of Pegg, Phillips and Barnett [20] was originally proposed for preparing superposition of vacuum and one-photon state by truncating a coherent light, but can readily be applied to generate superposition of vacuum, one-photon and two-photon states (truncation up to $s = 2$) as discussed by Koniorczyk *et al.* [21]. The PPB-scissors, if applied recurrently, can also be used for truncation up to arbitrary value of s as proposed by Villas-Bôas *et al.* [23]. It is worth noting that the resources and optical elements of the scheme increase very much with the increase of the dimension of the output state. Thus, one can generate the output states truncated to an arbitrary value of s, but with the additional cost [23].

In the simplest case for $s=1$, the beam splitter BS1 in the PPB scheme, presented in Fig. 1(a), is fed by one-photon in one input port whereas the second port is left at vacuum. One of the output ports of this beam splitter is fed to the second beam splitter where it is mixed with the coherent light. The output modes of the second beam splitter are detected and the condition in which one photon is detected in one of the modes and none in the other mode corresponds to the conditional preparation of vacuum and one-photon states at the output of the first beam splitter. In a recent study [39], we have proposed an experimental scheme for the practical realization of the QSD scheme for state truncation taking into account the realistic description of single-photon-state generation and photon counting detectors. As was analyzed in [39,40], the original Pegg-Phillips-Barnett quantum scissors, shown in Fig. 1(a), can be implemented experimentally in a setup described schematically in Fig. 2. This scheme is based on the ideas developed Rarity *et al.* in [41]. It consists of a parametric down conversion crystal as the single-photon source, conventional photon counters for conditional measurement and 50:50 beam splitters for generation of entangled photon number states (BS1) and for the mixing of coherent state with the entangled state (BS2).

In general, the state $|\alpha\rangle_{(s)}$ generated by the PPB truncation of the input coherent state, given by (12), can be given by

$$|\alpha\rangle_{(s)} = \mathcal{N}_s \sum_{n=0}^{s} \frac{\alpha^n}{\sqrt{n!}} |n\rangle \tag{13}$$

normalized by

$$\mathcal{N}_s = \left(\sum_{n=0}^{s} \frac{|\alpha|^{2n}}{n!} \right)^{-1/2} = \left\{ (-1)^s L_s^{-s-1}(|\alpha|^2) \right\}^{-1/2}, \tag{14}$$

where $L_s^n(x)$ is the generalized Laguerre polynomial. The case for $s = 1$ was described in [20,39], for $s = 2$ in [21] and for any s in [23]. Equation (13) is just the Fock expansion (12) of the conventional ID CS truncated at the sth term and properly normalized. By definition, the PPB-truncated CS goes over into the Glauber CS in the limit of $s \to \infty$. Properties of the states were analyzed by Kuang *et al.* [16] and Opatrný *et al.* [18]. In order to calculate the Wigner function, we substitute Eq. (13) into Eq. (9), arriving at

$$W_s(n, \theta_m) = \frac{\mathcal{N}_s^2}{s+1} \left(\sum_{k=0}^{M} \frac{|\alpha|^M}{\sqrt{k!(M-k)!}} \exp[i(2k - M)(\theta_m - \varphi)] \right.$$
$$\left. + \sum_{k=M+1}^{s} \frac{|\alpha|^{M+s+1}}{\sqrt{k!(M-k+s+1)!}} \right), \tag{15}$$
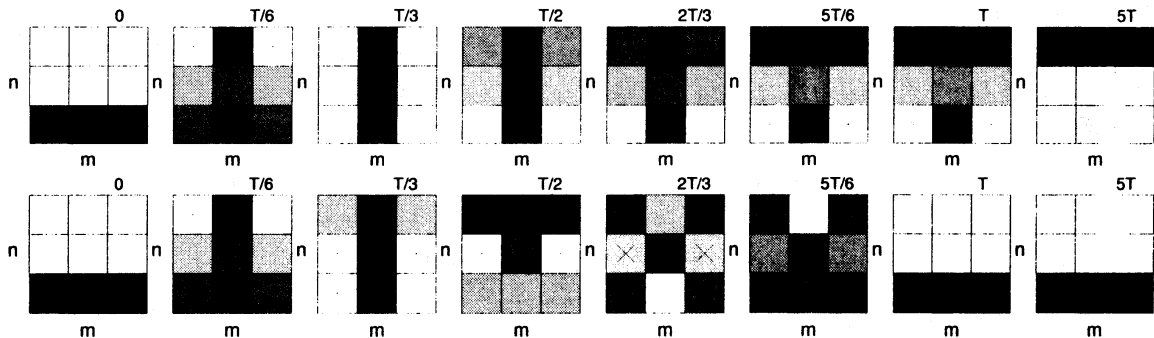
FIG. 3. Wigner function in 3-dimensional ($s = 2$) Hilbert space for the PPB-truncated (first row) and LT-truncated (2nd row) coherent states for different values of displacement parameter α chosen as fractions or multiples of the period $T \equiv T_2 = 2\pi/\sqrt{3}$. Brighter regions correspond to lower values of Wigner function, while the negative regions are marked additionally by crosses.
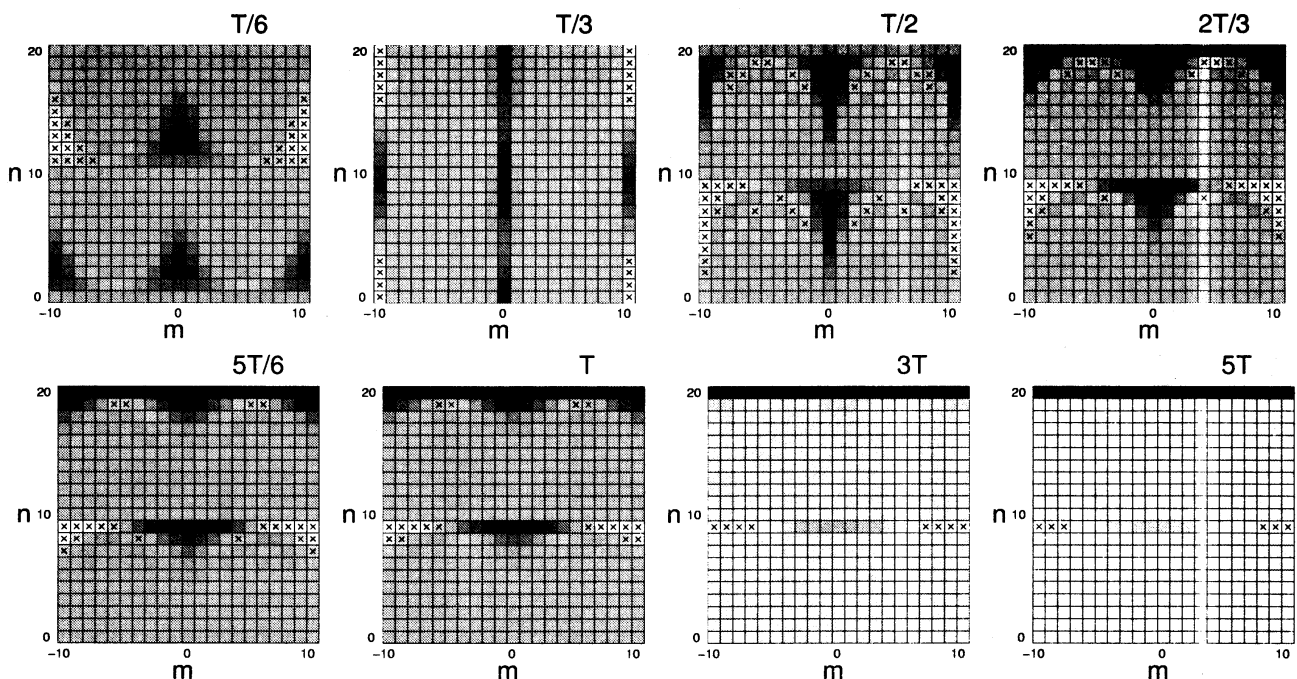

FIG. 4. Wigner function in 21-dimensional ($s = 20$) Hilbert space for the PPB-truncated coherent states for different values of displacement α being fractions or multiples of the quasiperiod $T \equiv T_{20} \approx 9.2$.

where $M = 2n \bmod(s + 1)$. It is worth noting that this approach is similar to the Vaccaro-Pegg formalism [34] of the Wigner function. Different shapes of the Wigner functions for various α are computed for $s=2$ in Fig. 3 and $s=20$ in Fig. 4. With $|\alpha|$ increasing from zero, the peak–antipeak transition occurs from $n = s$ to $n = 0$ around the value $|\alpha|^2 \approx s/2$ (corresponding to $|\alpha| \approx T_s/3$ in Fig. 4). However, if $|\alpha|^2 \gg s/2$, the situation is inverse: We observe two peaks for $n > s/2$ and a peak–antipeak structure for $n \leq s/2$ (for instance, $|\alpha| \approx 2T_s/3$ in Fig. 4). In the case when $|\alpha|^2 \approx s$ (Fig. 4 for $|\alpha| \approx T_s/2$), the W function has a more general shape. With increasing $|\alpha|$ the two-peak structure shifts to larger values of n, while the peak–antipeak structure gradually vanishes at $n \leq s/2$ (Fig. 4 for $|\alpha| = 2T_s/3, ..., 5T_s$). The shape is still comparatively simple. But by further increasing

$|\alpha| \gg T_s$, the Wigner function has a very simple structure representing the number state $|s\rangle$. Even for $|\alpha| = 25T_s$, as presented in Fig. 4, the peak–antipeak structure at $n \leq s/2$ vanishes almost completely. In the limit of $|\alpha|^2/s \to \infty$, the truncated CS approaches the number state $|s\rangle$.

B. QUANTUM SCISSORS OF LEOŃSKI AND TANAŚ

The optical truncation scheme of Leoński and Tanaś [24] was originally proposed for the generation of single-photon states, and then modified to describe n-photon state generation [25] and optical truncation [26,27]. The scheme in Fig. 1(b) describes a system, which can be governed by the following interaction Hamiltonian ($\hbar = 1$)

$$\hat{H} = \hat{H}_{\text{Kerr}} + \hat{H}_{\text{PGM}}, \tag{16}$$

where

$$\hat{H}_{\text{Kerr}} = \frac{\chi^{(s)}}{s+1}(\hat{a}^\dagger)^{(s+1)}\hat{a}^{(s+1)},$$

$$\hat{H}_{\text{PGM}} = \epsilon(\hat{a}^\dagger + \hat{a})\sum_m \delta(t - mT_{\text{kick}}). \tag{17}$$

Here, $\hat{H}_{\text{Kerr}}$ is the $(s+1)$-photon Kerr Hamiltonian [42] giving rise to optical bistability with $\chi^{(s)}$ denoting the nonlinearity constant; $\hat{H}_{\text{PGM}}$ describes the parametric gain medium pumped by an external classical pulsed field modelled as a train of delta functions; ϵ is the strength of the interaction with the external field; T_{kick} is the period of free evolution between each pump pulse (kick), and $\hat{a}^\dagger$ and $\hat{a}$ are bosonic creation and annihilation operators, respectively. All operators appearing in Eq. (16) are defined in the ID Hilbert space. As was shown in Refs. [26,27] by omitting terms of the order $\mathcal{O}(\epsilon^2)$, the state generated in the model (16) is of the form

$$|\alpha'\rangle_{(s)} = \exp(\alpha\hat{a}_s^\dagger - \alpha^*\hat{a}_s)|0\rangle, \tag{18}$$

where $\hat{a}_s$ and $\hat{a}_s^\dagger$ are, respectively, the FD annihilation and creation operators defined by (2). The states (18) generated in the Leoński-Tanaś scheme, referred to as the LT-truncated coherent states, are obtained by truncation of operators $\hat{a}_s$ and $\hat{a}_s^\dagger$. Their physical properties in relation to the Pegg-Barnett phase formalism [38] were analyzed in Refs. [15,17,18]. To show the differences between the PPB- and LT-truncated states, we present the explicit Fock expansion of (18) in the form [17]

$$|\alpha'\rangle_{(s)} = \sum_{n=0}^{s} e^{in\varphi} b_n^{(s)} |n\rangle, \tag{19}$$

where

$$b_n^{(s)} = \frac{s!}{s+1}\frac{(-i)^n}{\sqrt{n!}}\sum_{k=0}^{s} e^{ix_k|\alpha|}\frac{\text{He}_n(x_k)}{\text{He}_s^2(x_k)}. \tag{20}$$

Here, $x_k \equiv x_k^{(s+1)}$ are the roots, $\text{He}_{s+1}(x_k) = 0$, of the Hermite polynomial $\text{He}_n(x) \equiv 2^{-n/2}H_n(x/\sqrt{2})$. In the special case for $s = 1$, the LT-truncated CS reduces to
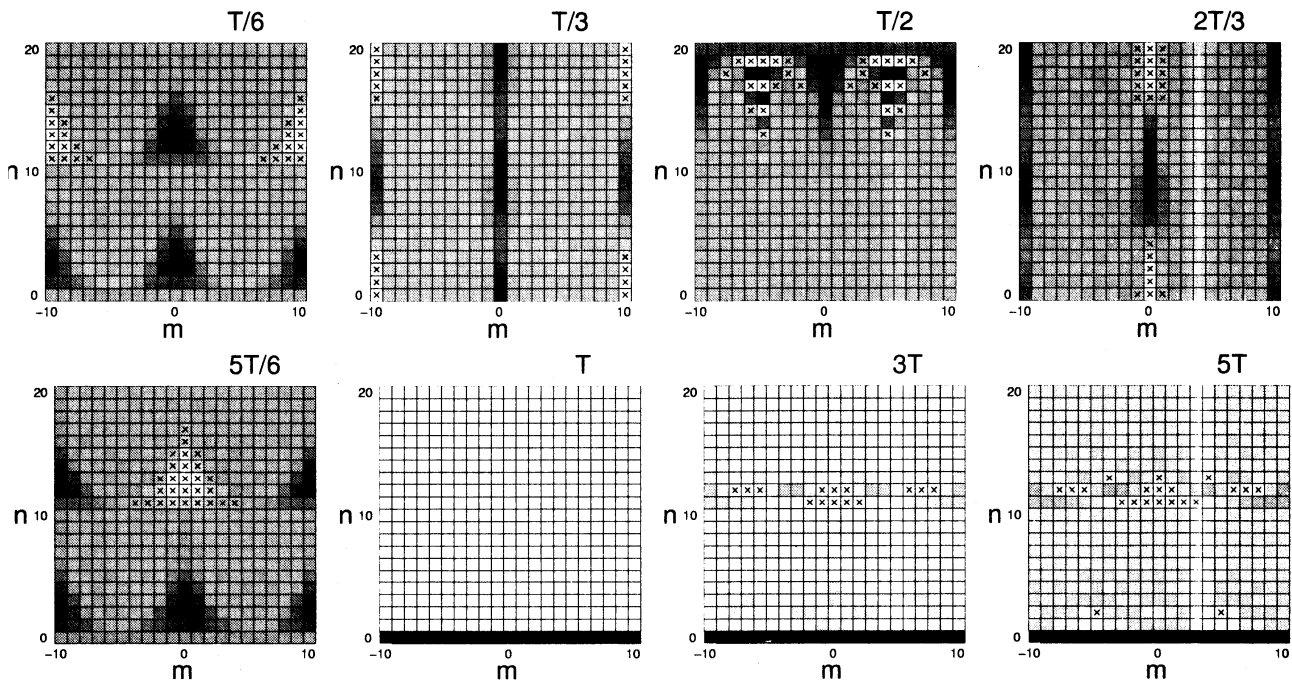
FIG. 5. Same as in Fig. 4, but for the LT-truncated coherent states.

$|\alpha'\rangle_{(1)} = \cos|\alpha||0\rangle + e^{i\varphi}\sin|\alpha||1\rangle$. It is seen that $|\alpha'\rangle_{(1)}$ is periodic in α. The LT-truncated CS goes over into the conventional CS in the limit of $s \to \infty$. As was shown in [17], $|\alpha'\rangle_{(s)}$ are periodic in $|\alpha|$ for $s=1$, 2 and approximately periodic (referred to as the quasiperiodic) for higher values of s. This property can be well described by analyzing Wigner functions for the LT-truncated CS.

On insertion of the coefficients (19) into the general formula (9), we get the Wigner function for $|\alpha\rangle_{(s)}$ in the form

$$W_s(n,\theta_m) = \sum_{k=M+1}^{s} \frac{\exp[i(2k - M - s - 1)(\theta_m - \varphi + \pi/2)]}{[k!(M - k + s + 1)!]^{1/2}} G_{1k}$$

$$+ \sum_{k=0}^{M} \frac{\exp[i(2k - M)(\theta_m - \varphi + \pi/2)]}{[k!(M - k)!]^{1/2}} G_{0k}, \qquad (21)$$

where

$$G_{\eta k} = \frac{(s!)^2}{(s+1)^3} \sum_{p=0}^{s} \sum_{q=0}^{s} \exp[i(x_q - x_p)|\alpha|] \frac{He_k(x_p)He_{M-k+\eta(s+1)}(x_q)}{[He_s(x_p)He_s(x_q)]^2} \qquad (22)$$

with $\eta = 0, 1$. The periodicity of $|\alpha'\rangle_{(2)}$ is clearly seen in the Wigner function given in the 2nd row of Fig. 3 for $|\alpha| = 0, T_2, 5T_2$, where $T_2 = 2\pi/\sqrt{3}$. Let us analyze in greater detail the Wigner functions presented in Fig. 5 for $s = 20$. We observe the following behavior: The shape of the respective graph is quasiperiodic in the parameter $|\alpha|$ with quasiperiod $T_{20} \approx 9.2$. We find that for small $|\alpha|$ the shape is essentially the same as that described in Fig. 4 for the PPB-truncated CS — for $n \leq s/2$ (compare Figs. 4 and 5 for $|\alpha| = T_s/6$), there are two peaks of opposite phases, whereas for $n > s/2$ we observe a peak and an antipeak. Note, the peaks at the borders are artificially split up in our Cartesian representation of the

Wigner function. The peaks or antipeaks are located at such positions that on summing the W function with constant n (or θ_m) over θ_m (or n), we get the probability distribution of n (or θ_m , respectively). Then, with increasing $|\alpha|$, interesting oscillations in photon number appear. Their culmination is at $|\alpha| = T_s/2$, where only even photon numbers are present. For this value of α, the LT-truncated coherent state approaches an even CS, namely, the case of a Schrödinger cat state. By further enlarging $|\alpha|$, the W function returns to its previous shapes through the transition regime (for $|\alpha| \approx 2T_s/3$) to the case of the inner two-peak and outer peak–antipeak structure, similar to the Vaccaro–Pegg results. For $|\alpha| \approx 5T_s/6$, the W function is very similar to that for $|\alpha| \approx T_s/6$, but with opposite phase. Finally, for $|\alpha| = T_s$, we arrive at an almost vacuum state. By further increasing $|\alpha|$, these shapes of the W function graph reappeared for several quasiperiods T_s. Similar behavior can be observed also for other values of s. The mathematical explanation of the quasiperiodicity together with the formulas for the quasiperiod T_s were given in [18].

It is worth noting that all the states (except for vacuum) in Figs. 3–5 are purely quantum as finite superpositions of photon-number states. Their discrete Wigner functions can be negative (as marked by crosses in figures) for some values of photon numbers n and phases θ_m. Nevertheless, as for the standard continuous Wigner function, there can be highly-nonclassical states described by the completely positive discrete Wigner functions. For example, the W functions for the PPB-truncated states in Figs. 3–4 are entirely positive, in particular, at $\alpha = 5T_s$ which corresponds to the approximate s-photon Fock states. (They become the *exact* s-photon Fock states in the limit of $|\alpha| \to \infty$.)

IV. CONCLUSIONS

We contrasted two different formal approaches to define quantum optical states, by example of coherent states, in finite-dimensional Hilbert spaces. We discussed physical implementations of the quantum scissors for generation of the FD coherent states via optical truncation: (i) the scheme of Pegg, Phillips and Barnett [20] realized by projection synthesis in linear-optical system and (ii) the scheme of Leoński and Tanaś [24,26] based on a kicked dynamics of nonlinear-optical system. The distinct properties of the PPB and LT truncated coherent states were compared with the help of the discrete Wigner function. We have demonstrated that the PPB coherent states truncated at the s-photon state $|s\rangle$ are aperiodic in the amplitude $|\alpha|$ of the input coherent state, and they tend to $|s\rangle$ in the limit of $|\alpha| \to \infty$. By contrast, the $|\alpha|$-limit of the LT truncated coherent states is undetermined, since the states are periodic or quasiperiodic in $|\alpha|$ for finite s. The physical reason of this (quasi)periodicity for the states generated by the LT scheme and aperiodicity of those for the PPB scheme is related to (non)linearity of the systems. The PPB scheme is based on linear-optical elements thus cannot lead to states periodic in $|\alpha|$. However, the LT scheme utilizes the nonlinear-optical elements thus can generate periodic or quasiperiodic states in $|\alpha|$. Finally, we note the LT and PPB coherent states approach the same standard coherent states in the limit of s for any finite value of amplitude of the input field.

V. ACKNOWLEDGMENTS

[1] H. Weyl, *Theory of Groups and Quantum Mechanics* (Dover, New York, 1931).

[2] J. Schwinger, Proc. Natl. Acad. Sci. (USA) **46**, 570 (1960).

[3] J. M. Radcliffe, J. Phys. A **4**, 313 (1971).

[4] A. M. Perelomov, Commun. Math. Phys. **26**, 222 (1972); *Generalized Coherent States and their Applications* (Springer, Berlin, 1986).

[5] C. Arecchi, E. Courtens, R. Gilmore and H. Thomas, Phys. Rev. A **6**, 2211 (1972).

[6] R. Gilmore, Ann. Phys. (N.Y.) **74**, 391 (1972); Rev. Mex. Fis. **23**, 142 (1974); J. Math. Phys. **15**, 2090 (1974).

[7] W. M. Zhang, D. H. Feng, and R. Gilmore, Rev. Mod. Phys. **62**, 867 (1990).

[8] T. S. Santhanam and A. R. Tekumalla, Found. Phys. **6**, 583 (1976); T. S. Santhanam, Phys. Lett. A **56**, 345 (1976).

[9] R. J. Glauber and F. Haake, Phys. Rev. A **13**, 357 (1976).

[10] R. J. Glauber, Phys. Rev. **130**, 2529 (1963); *ibid.* **131**, 2766 (1963).

[11] E. C. G. Sudarshan, Phys. Rev. Lett. **10**, 277 (1963).

[12] Special issue on quantum state preparation and measurement, J. Mod. Opt. **44** (11/12) (1997).

[13] U. Leonhardt, Phys. Rev. Lett. **74**, 4101 (1995); *ibid.* **76**, 4293 (1996); Phys. Rev. A **53**, 2998 (1996); V. I. Man'ko, O. V. Man'ko, JETP **85**, 430 (1997); V. A. Andreev, V. I. Man'ko, JETP **87**, 239 (1998); V. Bužek, G. Drobný, G. Adam, R. Derka, P. L. Knight, J. Mod. Opt. **44**, 2607 (1997); R. Walser, J. I. Cirac, P. Zoller, Phys. Rev. Lett. **77**, 2658 (1996); J. -P. Amiet and S. Weigert, J. Phys. A **31** L543 (1998); *ibid.* **32** L269 (1999).

[14] A. Miranowicz, W. Leoński, and N. Imoto, in *Modern Nonlinear Optics*, ed. M. W. Evans, Adv. Chem. Phys., vol. 119 (I) (Wiley, New York, 2001) p. 155.

[15] V. Bužek, A. D. Wilson-Gordon, P. L. Knight, and W. K. Lai, Phys. Rev. A **45**, 8079 (1992).

[16] L. M. Kuang, F. B. Wang, and Y. G. Zhou, Phys. Lett. A **183**, 1 (1993); J. Mod. Opt. **41**, 1307 (1994).

[17] A. Miranowicz, K. Piątek, and R. Tanaś, Phys. Rev. A **50**, 3423 (1994).

[18] T. Opatrný, A. Miranowicz, and J. Bajer, J. Mod. Opt. **43**, 417 (1996).

[19] B. Roy and P. Roy, J. Phys. A **31**, 1307 (1998).

[20] D. T. Pegg, L. S. Phillips, and S. M. Barnett, Phys. Rev. Lett. **81**, 1604 (1998); S. M. Barnett and D. Pegg, Phys. Rev. A **60**, 4965 (1999).

[21] M. Koniorczyk, Z. Kurucz, A. Gabris, and J. Janszky, Phys. Rev. A **62**, 013802 (2000).

[22] M. G. A. Paris, Phys.Rev. A **62**, 033813 (2000).

[23] C. J. Villas-Bôas, Y. Guimarães, M. H. Y. Moussa, and B. Baseia, Phys. Rev. A **63**, 055801 (2001).

[24] W. Leoński and R. Tanaś, Phys. Rev. A **49**, R20 (1994).

[25] W. Leoński, Phys. Rev. A **54**, 3369 (1996); W. Leoński, S. Dyrting, and R. Tanaś, J. Mod. Opt. **44**, 2105 (1997).

[26] W. Leoński, Phys. Rev. A **55**, 3874 (1997).

[27] A. Miranowicz, W. Leoński, S. Dyrting, and R. Tanaś, Acta Phys. Slov. **46**, 451 (1996).

[28] W. Leoński, and A. Miranowicz, in *Modern Nonlinear Optics*, ed. M. W. Evans, Adv. Chem. Phys., vol. 119 (I) (Wiley, New York, 2001) p. 195.

[29] E. P. Wigner, Phys. Rev. **40**, 749 (1932); for a review, see M. Hillery, R. F. O'Connell, M. O. Scully, and E. P. Wigner, Phys. Rep. **106**, 121 (1984); V. I. Tatarskii, Sov. Phys. Usp. **26**, 311 (1983).

[30] R. L. Stratonovich, Sov. Phys. JETP **4**, 891 (1957); L. Cohen and M. O. Scully, Found. Phys. **16**, 295 (1986).

[31] R. F. O'Connell, and E. P. Wigner, Phys. Rev. A **30**, 2613 (1984).

[32] W. K. Wootters, Ann. Phys. **176**, 1 (1987).

[33] O. Cohendet, P. Combe, M. Sirugue, and M. Sirugue-Collin, J. Phys. A **21**, 2875 (1988).

[34] J. A. Vaccaro and D. T. Pegg, Phys. Rev. A **41**, 5156 (1990).

[35] A. Lukš and V. Peřinová, Phys. Scr. T **48**, 94 (1993).

[36] J. H. Hannay and M. V. Berry, Physica D **1**, 267 (1980).

[37] A. Luis and J. Peřina, J. Phys. A **31**, 1423 (1998).

[38] D. T. Pegg, and S. M. Barnett, Phys. Rev. A **41**, 3427 (1989).

[39] Ş. K. Özdemir, A. Miranowicz, M. Koashi, and N. Imoto, Phys. Rev A **64**, 063818 (2001).

[40] Ş. K. Özdemir, A. Miranowicz, M. Koashi, and N. Imoto, J. Mod. Opt. **49**, 977 (2002).

[41] J. G. Rarity and P. R. Tapster, Phys. Rev. A **59**, R35 (1999); Philos. Trans. R. Soc. London, Ser. A **355**, 2267 (1997); J. G. Rarity, P. R. Tapster, and R. Loudon, e-print quant-ph/9702032 (1997).

[42] C. C. Gerry, Phys. Lett. A **124**, 237 (1987); V. Bužek and I. Jex, Acta Phys. Slov. **39**, 351 (1989); M. Paprzycka and R. Tanaś, Quantum Opt. **4**, 331 (1992).